Geophysical Research Letters

RESEARCH LETTER
10.1029/2019GL082571

Hydrodynamic Controls on Primary Producer Communities in Spring-Fed Rivers

N. G. F. Reaver[1], D. A. Kaplan[1], R. A. Mattson[2], E. Carter[2], P. V. Sucsy[2], and T. K. Frazer[3,4]

[1]Department of Environmental Engineering Sciences, University of Florida, Gainesville, FL, USA, [2]St. Johns River Water Management District, Palatka, FL, USA, [3]School of Natural Resources and Environment, University of Florida, Gainesville, FL, USA, [4]Fisheries and Aquatic Sciences Program, School of Forest Resources and Conservation, University of Florida, Gainesville, FL, USA

Key Points:
- Flow velocity exerts a strong control on periphyton abundance but not macrophyte or macroalgae abundance
- Periphytic algal cover can expand rapidly when velocity decreases but is quickly removed when velocity is restored and is not hysteretic
- Periphytic algae likely exhibit threshold velocity behavior due to mechanical removal at the onset of continuous macrophyte canopy motion

Supporting Information:
- Supporting Information S1
- Movie S1
- Movie S2
- Movie S3
- Data Set S1
- Data Set S2
- Data Set S3

Correspondence to:
D. A. Kaplan,
dkaplan@ufl.edu

Citation:
Reaver, N. G. F., Kaplan, D. A., Mattson, R. A., Carter, E., Sucsy, P. V., & Frazer, T. K. (2019). Hydrodynamic controls on primary producer communities in spring-fed rivers. *Geophysical Research Letters*, *46*, 4715–4725. https://doi.org/10.1029/2019GL082571

Received 22 FEB 2019
Accepted 18 APR 2019
Accepted article online 24 APR 2019
Published online 11 MAY 2019

Abstract In many spring-fed rivers, benthic macroalgae and periphytic algae are increasing and, in some cases, replacing rooted vascular plants, which are critical to ecosystem function. While most research has focused on the role of nutrients in driving this change, in-channel hydrodynamics also control vascular plant and algal abundances and their interactions. Understanding relationships between hydrology and primary producers is essential for developing ecologically relevant flow regulations. We investigated the relationship between flow velocity and primary producer abundance in spring-fed rivers using observational data from 16 springs to determine critical velocity thresholds for periphyton, macroalgae, and vascular plants. We also used flow suppression experiments to quantify periphyton growth rates and test for hysteretic behavior. Results suggest a critical velocity of 0.22 m/s (95% CI: 0.13–0.28 m/s) for periphyton but no specific thresholds for macroalgae or vascular plants. Experimental and theoretical results supported these findings and suggest periphyton establishment is not hysteretic.

Plain Language Summary Spring-fed rivers are ecologically, socially, and economically important ecosystems. In many springs, algae has been increasing—and in some cases replacing —submerged plants, with negative ecosystem impacts. Restoring springs requires an improved understanding of the drivers of plant and algae abundance. In this study, we investigated the relationship between the speed of flowing water and the abundance of plant and algae using two approaches. First, we used observations of water speed and plant and algal abundances from 16 springs to determine if there was a critical flow speed above which plants and algae decreased. Second, we performed field experiments where we artificially reduced water speed, allowing algae to grow on submerged plants, and then quantified its growth and removal rates. The observational study showed that algae growing on plants (periphyton) is reduced at flow speeds above ~0.22 m/s. In contrast, submerged plants and algae growing on the river bottom did not have identifiable thresholds. The experimental study and theoretical calculations agreed with these results and identified the mechanism for this threshold. Finally, we found that increased algae abundance returns to its previous state when flow is restored, suggesting that restoring water flows can also help reduce algal levels in impacted springs.

1. Introduction

Globally, lotic ecosystems face degradation from flow reduction, nutrient and contaminant pollution, invasive species introduction, channel and floodplain modification, and other anthropogenic drivers (Malmqvist & Rundle, 2002). Changes in primary producer community structure (PPCS) are a highly visible and fundamental symptom of ecosystem disturbance (Townsend et al., 2017) and have motivated intensive river restoration efforts in recent decades (Bernhardt et al., 2005; Wohl et al., 2015). A substantial portion of restoration efforts do not achieve their desired results (Kail et al., 2015) however, highlighting the need for improved understanding of physical-biotic interactions in lotic systems and the development of general methodologies for their elucidation. In particular, understanding how flow regime structures PPCS in lotic ecosystems is critical for attributing causal mechanisms of observed ecological change and setting flow management or restoration goals.

Hydrodynamics is known to play an important role in shaping primary producer communities in rivers and streams (Biggs, 1996; Biggs & Stokseth, 1996; Franklin et al., 2008; Jowett & Biggs, 2010). Higher flow velocities can increase nutrient delivery by thinning the diffusive boundary layer over primary producer

surfaces, increasing their productivity (Biggs, 1996; Biggs & Stokseth, 1996; Larned et al., 2004; Nepf, 2012a, 2012b; Saravia et al., 1998). However, if velocities are too high, primary producers can be dislodged from the substrate or prevented from colonizing (Franklin et al., 2008; Ghosh & Gaur, 1998; Ryder et al., 2006; Wellnitz & Rader, 2003). Primary producers also exert control on the structure of lotic ecosystems, modifying both their hydrodynamics and morphology through complex flow-vegetation-sediment feedbacks (Gurnell, 2014). Lotic primary producers include rooted vascular plants (VP), macroalgae, and periphyton (O'Hare, 2015), and for all communities, biomass is generally negatively correlated with velocity (Biggs, 1996; Biggs & Stokseth, 1996). As such, changes in velocity driven by natural or human-induced flow alterations have the potential to drive substantial variation in PPCS, a phenomenon that has been widely observed in Florida (USA) springs.

Springs are highly productive, clear-water ecosystems fed by groundwater discharge (Scott et al., 2004). Compared to surface water-fed systems, springs have extremely stable discharge, temperature, and chemical composition, making them excellent settings for controlled experiments (Heffernan et al., 2010; Odum, 1957). Florida has one of the highest concentrations of springs in the world (FSTF, 2000), and these unique ecosystems represent a vital ecological, cultural, and economic resource (Bonn & Bell, 2003; Borisova et al., 2014; Dunbar et al., 1989; Huth & Morgan, 2011; Laist & Reynolds, 2005). Florida's springs were historically dominated by VP (primarily *Vallisneria americana* and *Sagittaria kurziana*), but benthic and periphytic algae are increasing in a majority of springs (Stevenson et al., 2004), substantially shifting PPCS and associated ecological and recreational functions (Foss et al., 2012). Notably, these shifts have occurred contemporaneously with observed increases in nitrogen concentration and declines in the discharge of many springs (FSTF, 2000).

Understanding the root cause(s) of observed PPCS shifts is vital for springs restoration and management, and multiple plausible hypotheses have been advanced (Heffernan et al., 2010; Hensley & Cohen, 2017; Liebowitz et al., 2014). One potential driver is hydraulic control of algal abundance, specifically the ability of flow velocity to limit or prevent algal colonization, establishment, and accumulation. In this work, we investigated hydrodynamic control of PPCS using complementary observational, experimental, and theoretical methodologies. We hypothesized that if velocity exerts a consistent control on primary producer abundance, the effect will be evident in field observations across multiple springs. We tested this by applying a critical threshold velocity model to observational data sets of VP, macroalgae, periphyton, and velocity from 16 Florida springs. Additionally, we manipulated velocity in one spring (Silver River, FL) to experimentally verify threshold velocities for periphyton, quantify periphyton growth dynamics and test for hysteretic effects (i.e., whether algal abundance returned to initial levels after flow manipulation ceased). Finally, we applied a physical model to describe a plausible mechanism for the existence of critical velocity thresholds.

2. Data and Methods

2.1. Observational and Experimental Data Sets

Observational data sets from five separate studies involving 16 springs were used to identify critical velocity thresholds, if present, for VP, macroalgae, and periphyton abundance. Specific data formats varied among data sets; however, all studies included primary producer abundance and flow velocity measurements, which were harmonized as described in section 2.2 and the supporting information (SI). The five studies were (1) the Gulf Coast Springs Survey, containing periphyton, macroalgae, and VP data from three springs from 2003 to 2011 (Canfield & Hoyer, 1988; Frazer et al., 2001, 2006; Hoyer et al., 2004; Moss, 1976); (2) the Gum Slough Filamentous Algae Survey, containing macroalgae data from one spring from 2010 to 2013 (King, 2014); (3) the Synoptic Biological Springs Study, containing periphyton, macroalgae, and VP data from 14 springs from 2015 (AFW, 2016); (4) the Collaborative Research Initiative on Sustainability and Protection of Springs (CRISPS) Submerged Aquatic Vegetation Groundtruthing Survey, containing periphyton and VP data from one spring from 2014 to 2016; and (5) the CRISPS Hydraulics and Hydrodynamics Periphyton Survey, containing periphtyon data from one spring from 2017. A complete description of each data set is given in Text S1.

Experimental data were derived using in situ flow manipulation structures to reduce velocity in a section of the Silver River, observing the rate of periphyton growth or colonization on VP in areas with suppressed

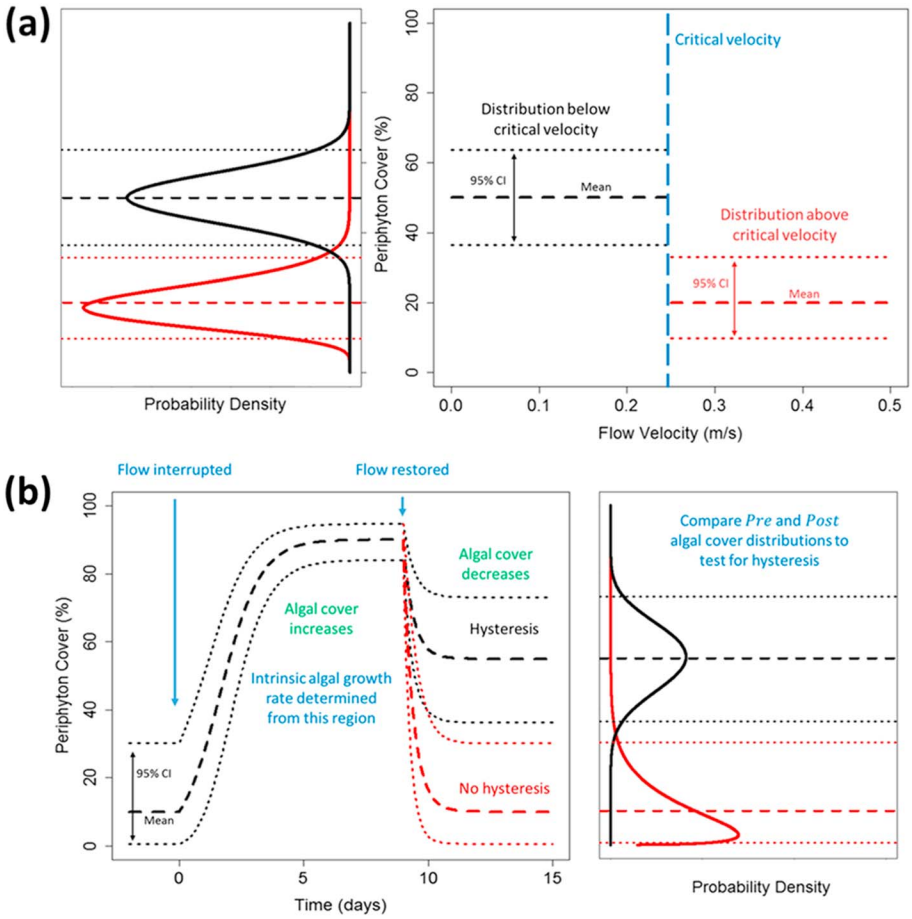

Figure 1. (a) Conceptual summary of the critical velocity threshold model. One primary producer abundance distribution (in this case algal percent cover) exists below the critical velocity (black), while a different distribution exists above this velocity (red). (b) Conceptual summary of the periphyton growth dynamics model and test for hysteresis. Flow is interrupted at time 0, after which periphyton abundance increases logistically from its initial value, A_0, to the carrying capacity, K. When flow is restored, periphyton abundance is reduced. Comparison of periphyton abundance distributions before and after flow modification indicates potential hysteretic behavior.

velocity (and paired controls without flow manipulation), and then restoring flow and measuring periphyton loss. The structure diverted flow above and around its footprint, effectively reducing velocity behind the structure to 0, without blocking light (Figures S1 and S2 and Movie S1). Structures were deployed at 19 sites in the Silver River across gradients of velocity and VP/periphyton cover. During each deployment, periphytic algal cover on VP was measured using digital photography ($n = 6$ images per site, per sampling event, maximum sampling interval of 2 days). After 1 week, flow was restored, and periphyton cover was measured using the same procedure. Periphyton abundance was quantified by randomizing the order of images and visually assigning each an abundance of "very low," "low," "medium," "high," or "very high" (Text S1). This post-field ranking methodology mitigates potential observer bias or error present when using other defined-threshold categorization schemes, such as Braun-Blanquet classification (Wikum & Shanholtzer, 1978), or estimating cover directly (Klimeš, 2003; Lepš & Hadincová, 1992).

2.2. Estimating Critical Velocity Thresholds From Observational Data

We applied a critical threshold velocity model that tests whether two distinct primary producer abundance distributions exist above and below a critical velocity threshold (Figure 1a). Any measure of primary producer abundance could be used for this test; here we use algal percent cover (A) based on the availability of these data across all studies. The distribution of A can be written as

$$A \sim \begin{cases} \beta[\mu_1, {\sigma_1}^2], & v < v_c \\ \beta[\mu_2, {\sigma_2}^2], & v > v_c \end{cases} \quad (1)$$

where $\beta[\mu_1, {\sigma_1}^2]$ is a Beta distribution with mean, μ_1, and variance, ${\sigma_1}^2$, for flow velocities, v, below the critical threshold velocity, v_c. Similarly, $\beta[\mu_2, {\sigma_2}^2]$ is a Beta distribution with mean, μ_2, and variance, ${\sigma_2}^2$, for v above v_c. We used the Beta distribution for A since it has finite support between 0 and 1, which corresponds to the 0% to 100% range for A. Using the Heaviside step function, $\Phi(\ )$, we can rewrite equation (1) as a single distribution with its parameters $\mu(v)$ and $\sigma^2(v)$ as functions of v,

$$\begin{aligned} A(v) &\sim \beta[\mu(v), \sigma^2(v)] \\ \mu(v) &= \mu_1 \Phi(v) + (\mu_2 - \mu_1)\Phi(v - v_c) \\ \sigma^2(v) &= {\sigma_1}^2 \Phi(v) + ({\sigma_2}^2 - {\sigma_1}^2)\Phi(v - v_c) \end{aligned} \quad (2)$$

Equation (2) is illustrated conceptually in Figure 1a. A form of equation (2) was used for all observational data sets that quantified VP/algal abundance in terms of cover, while an analogous form was used for those that measured algal biomass (see SI).

We used Bayesian statistical inference to calibrate equation (2) for each of the observational data sets, resulting in probability distributions for each of the model parameters (v_c, μ_1, ${\sigma_1}^2$, μ_2, and ${\sigma_2}^2$), for each data set. When calibrating equation (2) to N values of algal abundance and flow velocity observations (i.e., $\{A_i\}$,$\{v_i\}$), Bayes theorem can be written as

$$p\left(v_c, \mu_1, {\sigma_1}^2, \mu_2, {\sigma_2}^2 | \{A_i\}, \{v_i\}\right) \propto \left(\prod_{i=1}^{N} \beta[A_i | \mu(v_i), \sigma^2(v_i)] \right) p(v_c) p(\mu_1) p\left({\sigma_1}^2\right) p(\mu_2) p\left({\sigma_2}^2\right) \quad (3)$$

where $\beta[A_i|\mu(v_i), \sigma^2(v_i)]$ is the likelihood of a single abundance observation, A_i, given the corresponding v_i and equation (2); and $p(...)$ are the prior probability distributions for each parameter (e.g., $p(v_c)$ is a uniform distribution). Explicit functional forms of the posterior distributions for each data set are given in the SI (Text S2). Posterior probability distributions were sampled using a random walk Metropolis-Hasting Gibbs Sampling algorithm (Text S2). One-dimensional marginal probability distributions for v_c for each observational data set were obtained from samples of corresponding multivariate posterior distributions. Overall estimates of v_c for each primary producer class (i.e., periphyton, macroalgae, and VP) were obtained by creating mixture distributions from all v_c marginal distributions for each class.

2.3. Quantifying Periphyton Growth Dynamics and Hysteresis From Experimental Data

We applied a logistic growth model to describe the growth dynamics of periphyton released from hydraulic control. The model assumes that the mean behavior of periphyton cover as a function of time, $A(t)$, is logistic and that variance around this mean follows a Beta distribution. Mathematically, this can be expressed as

$$\begin{aligned} A(t) &\sim \beta[\mu(t), \sigma^2] \\ \mu(t) &= \frac{K A_0 e^{rt}}{K + A_0(e^{rt} - 1)} \end{aligned} \quad (4)$$

where A_0 is the initial periphyton coverage, K is the carrying capacity, and r is the intrinsic growth rate. Equation (4) is illustrated conceptually in Figure 1b. We again used Bayesian statistical inference to calibrate equation (4) to periphyton abundance time series. Since periphyton abundance was quantified categorically (section 2.1), relative thresholds between categories were defined as explicit parameters (φ_1 φ_2, φ_3, and φ_4), which corresponded to the divisions between periphyton abundance categories. For this calibration, Bayes theorem is written as

$$p(A_0, K, r, \sigma^2, \varphi_1, \varphi_2, \varphi_3, \varphi_4 | N_1, \{t_{1,i}\}, N_2, \{t_{2,j}\}, N_3, \{t_{3,k}\}, N_4, \{t_{4,w}\}, N_5, \{t_{5,q}\}) \propto$$
$$\left(\prod_{i=1}^{N_1} I_{\varphi_1}\left[\mu(t_{1,i}), \sigma^2\right]\right)\left(\prod_{j=1}^{N_2} I_{\varphi_2}\left[\mu(t_{2,j}), \sigma^2\right] - I_{\varphi_1}\left[\mu(t_{2,j}), \sigma^2\right]\right)$$
$$\left(\prod_{k=1}^{N_3} I_{\varphi_3}\left[\mu(t_{3,k}), \sigma^2\right] - I_{\varphi_2}\left[\mu(t_{3,k}), \sigma^2\right]\right)\left(\prod_{w=1}^{N_4} I_{\varphi_4}\left[\mu(t_{4,w}), \sigma^2\right] - I_{\varphi_3}\left[\mu(t_{4,w}), \sigma^2\right]\right) \quad (5)$$
$$\left(\prod_{q=1}^{N_5} 1 - I_{\varphi_4}\left[\mu(t_{5,q}), \sigma^2\right]\right) p(A_0)p(K)p(r)p(\sigma^2)p(\varphi_1)p(\varphi_2)p(\varphi_3)p(\varphi_4)$$

where $I_x[\mu, \sigma^2]$ is the regularized incomplete Beta function (Text S2); N_1, N_2, N_3, N_4, and N_5 are the number of periphyton abundance observations of very low, low, medium, high, and very high, respectively; $\{t_{1,i}\}$, $\{t_{2,j}\}$, $\{t_{3,k}\}$, $\{t_{4,w}\}$, and $\{t_{5,q}\}$ are the corresponding timings of the periphyton abundance observations; and $p(...)$ are the prior probability distributions for each parameter. Explicit functional forms of each posterior distribution are given in the SI (Text S3).

Calibrated posterior probability distributions were used to quantify characteristics of periphyton growth, including the intrinsic doubling time, T_d,

$$T_d = \frac{\ln(2)}{r} \quad (6)$$

and growth potential, G_p,

$$G_p = K - A_0 \quad (7)$$

We used growth potential as an indicator of periphyton growth suppression when under hydraulic control, with high (unrealized) values indicating greater suppression. Overall estimates of T_d and K were obtained by creating mixture distributions from the marginal distributions of T_d and K for each deployment. Additionally, G_p estimates for each deployment were paired with corresponding pre-manipulation flow velocity to verify velocity thresholds derived from observational data.

To test for hysteresis in periphyton abundance, we compared abundance distributions before flow modification and several days after flow was restored (periphyton abundance quickly declined and stabilized after ~1 day; Movie S2). Figure 1b conceptually illustrates our approach. Periphyton abundance distributions can be written as

$$A_b \sim \beta\left[\mu_b, {\sigma_b}^2\right]$$
$$A_a \sim \beta\left[\mu_a, {\sigma_a}^2\right] \quad (8)$$

where b corresponds to *before* flow modification and a corresponds to *after* flow modification. Statistical difference was assessed by comparing the distributions of $\mu_b - \mu_a$ and ${\sigma_b}^2 - {\sigma_a}^2$ for each deployment. If the 95% credible intervals of $\mu_b - \mu_a$ or ${\sigma_b}^2 - {\sigma_a}^2$ contained 0, A_b and A_a were considered statistically indistinguishable, and no hysteretic effect was supported; if they did not contain 0, there was evidence for a hysteretic effect. Explicit functional forms of all posterior distributions are given in Text S3.

2.4. Threshold Velocity for VP Canopy Motion

One plausible physical mechanism for the existence of critical velocity thresholds for periphyton is a corresponding velocity threshold for VP canopy continuous motion. Since periphyton grows and accumulates on VP surfaces, it is susceptible to mechanical removal from abrasion as VP blades slide past one another. The frequency of contact-induced abrasive events increases dramatically when the VP canopy is in continuous motion (Doaré et al., 2004). Flexible VP canopy motion is known to be sustained by the generation of traveling vortices caused by Kelvin-Helmholtz instabilities, which can induce traveling waves within VP known as monami (Okamoto et al., 2016; Okamoto & Nezu, 2009; Patil & Singh, 2010) (Movie S3). Monami occur when the instantaneous drag force exerted by the vortices exceeds the buoyancy and rigidity of the VP (Nepf, 2012a), which has a well-defined physical threshold. Using conceptual frameworks, formulae, and

values from Ghisalberti and Nepf (2002, 2006), Nepf (1999, 2012a), and Ortiz et al. (2015), we derived an approximation (Text S4) of the minimum average mixing layer (i.e., turbulent layer above the VP canopy) velocity required for monami generation, v_m,

$$v_m \cong \left[\frac{1}{\Omega}\right] v_a = \left[\frac{1}{\Omega}\right]\left[\frac{2}{3}\right] v_i = \left[\frac{1}{1.4}\right]\left[\frac{2}{3}\right]\sqrt{\frac{E\tau^3}{3\rho_w C_S \delta_e \left(h-\frac{\delta_e}{2}\right)^2} + \frac{2\Delta\rho\tau g(\delta_e + 2h)}{3\rho_w C_S \delta_e}} \tag{9}$$

where v_a is the traveling velocity of the vortices; Ω is the ratio $\frac{v_a}{v_m}$, which ranges between 1 and 1.8; v_i is the maximum instantaneous velocity of a vortex, related to v_a by $v_a = \frac{2}{3} v_i$, $\delta_e = \frac{0.23\Delta S^2}{C_D W}$ and is the depth into which the vortices can penetrate the canopy; $C_S = 1.11 + 0.02\left(\frac{W}{\delta_e} + \frac{\delta_e}{W}\right)$ and is the drag coefficient of an individual VP blade; C_D is the bulk drag coefficient of the whole VP canopy, $\Delta\rho = (\rho_w - \rho_s)$; ρ_w is the density of water; ρ_s is the density of VP tissue; E is the Young's modulus of VP tissue; ΔS is the characteristic distance between VP blades; W is the characteristic VP blade width; h is the characteristic VP height; τ is the characteristic VP blade thickness; and g is the acceleration due to gravity. Equation (9) was parameterized using VP morphology data from the two CRISPS studies described above and (Hauxwell et al. (2007), Lei and Nepf (2016), Nepf (2012b), and Tanino and Nepf (2008), with resulting parameters, $C_D = 1$, $\rho_s = 850$ kg/m^3, $E = 0.883$ GPa, $\Delta S =$ 15.3 mm, $W =$ 12.0 mm, $h = 787$ mm, and $\tau =$ 0.7 mm. Estimates of v_m were then compared to critical velocity threshold estimations for periphyton abundance from observational and experimental data.

3. Results

Observational critical velocity threshold analyses are summarized in Figure 2. Representative model calibrations for each primary producer class (periphyton, macroalgae, and VP) are given in Figures 2a–2c, and Figures 2d–2f summarize v_c estimates across all data sets for each class. Periphyton showed a clear velocity threshold, exemplified both by the sharp decline in median primary producer abundance (red line in Figure 2a) as well as by the relatively narrow 95% credible interval (0.13–0.28 m/s) around the overall median periphyton v_c (0.22 m/s) across studies (Figure 2d). In contrast, there was no clear velocity threshold for macroalgae or VP (Figures 2b and 2c), and v_c for these classes had 95% credible intervals that encompassed nearly the entire velocity range in the data sets (0.02–0.63 m/s for macroalgae and 0.02–0.61 m/s for VP).

Figures S3 and S4 show an example of the digital images and logistic growth model calibrated to periphyton abundance data from one deployment of the flow suppression experiment, illustrating that periphyton abundance at the control sites remained essentially unchanged throughout the deployment, while it increased dramatically at treatment sites. Results from all flow suppression experiments are summarized in Figure 3. Figure 3a shows G_p as a function of velocity for all deployments and illustrates a distinct transition between lower and higher values of G_p near 0.2 m/s, similar to the finding of median $v_c = 0.22$ m/s for periphyton abundance in the observational study. Figures 3b and 3c summarize results for periphyton T_d and K, which were estimated at 0.64 days (95% CI: 0.14 to 2.3 days) and 82% cover (95% CI: 45–98%), respectively. Hysteresis analysis revealed that only 3 of 19 deployments showed statistically distinguishable periphyton distributions before and after the flow manipulation; two had significantly more periphyton after the manipulation, and one had significantly less (Table S2). Finally, we estimated a mean monami generation velocity threshold, v_m, of 0.23 m/s, with a range between 0.13 and 0.33 m/s for sparse and dense VP canopies, respectively.

4. Discussion

Flow has been described as a "master variable" (Poff et al., 1997) that controls the fundamental physical, energetic, and biological characteristics of lotic ecosystems (Naiman et al., 2008; Poff et al., 2010). Alterations in riverine flow regimes have wide-ranging physical, chemical, and biological effects (Richter et al., 1996) at the point- (Song et al., 2018) to whole-river (Timpe & Kaplan, 2017) scales. Flow magnitude directly effects riverine eco-hydraulics through interactions among primary producers, sediments, channel morphology, and local-scale hydrodynamics (Gurnell, 2014; Larsen & Harvey, 2010; Murray et al., 2008; Nepf, 2012a). Systems with altered flow regimes can thus undergo rapid ecological change, including the loss of vegetated features (Heffernan, 2008), degradation of ecosystem patterning (Casey et al., 2016), and alteration of primary producer and associated invertebrate assemblages (Choudhury et al., 2015); these changes

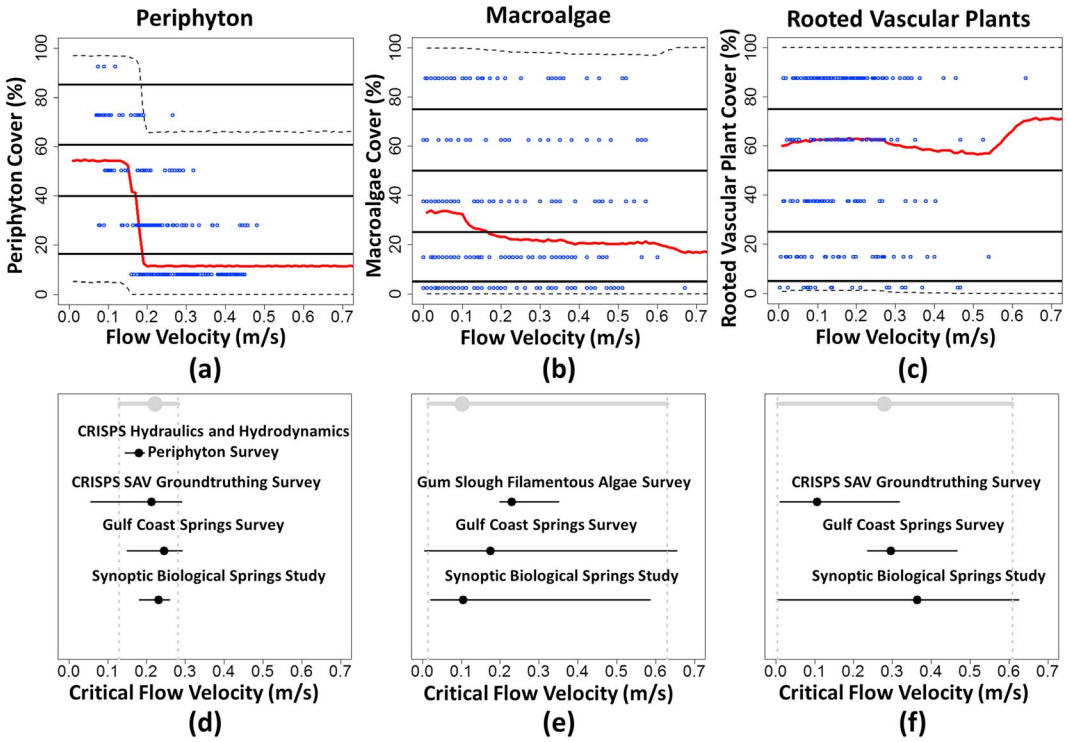

Figure 2. Summary of observational critical velocity threshold results. (a, b, and c) Representative critical threshold velocity model calibrations for periphyton (CRISPS Hydraulics and Hydrodynamics Periphyton Survey), macroalgae (Gulf Coast Springs Survey), and VP (Synoptic Biological Springs Study), respectively. The solid red lines represent median primary producer abundance, and the dotted black lines represent 95% credible intervals. Solid black horizontal lines give the thresholds between the visual classification values. (d, e, and f) The medians with 95% credible intervals for v_c across all observational data sets (black) and the overall mixture distribution (gray) for periphyton, macroalgae, and VP, respectively. CRISPS = Collaborative Research Initiative on Sustainability and Protection of Springs; SAV = Submerged Aquatic Vegetation.

are often associated with transitions to states that are resistant to restoration (Corenblit et al., 2007). In this context, understanding the physical-biotic interactions controlling PPCS is vital for successful management and restoration of lotic ecosystems.

In this study, we synthesized and analyzed paired observations of abundance and velocity from 16 springs for three primary producer classes, finding that periphyton abundance had a distinct critical velocity threshold (Figure 2d), while benthic macroalgae and VP did not (Figures 2e and 2f). This consistency across 16 springs, using a variety of data collection methods, suggests that 0.22 m/s (95% CI: 0.13–0.28 m/s) does indeed represent a significant hydraulic-driven control on periphyton abundance. In contrast, macroalgae and VP abundance did not appear to have well-defined velocity-driven controls, a finding that is at odds with several previous studies. Specifically, Hoyer et al. (2004) observed substantial reductions in macroalgae and VP biomass at velocities >0.25 m/s, Riis and Biggs (2003) found VP abundance declined at velocities >0.40 m/s (measured in vegetation-free zones), King (2014) found macroalgal cover to decrease substantially for velocities >0.22 m/s, and Nilsson (1987) found VP species richness declines for velocities >0.48 m/s.

The lack of well-constrained macroalgae and VP velocity thresholds in our study does not necessarily indicate an absence of hydraulic-driven control for these classes, only that critical threshold velocities were not statistically identifiable across these 16 springs within the range of observed velocities. These findings could be due to a genuine lack of control in this velocity range or may be driven by interactions among location-dependent hydraulic controls. Notably, many hydraulic-driven controls on primary producer abundance (e.g., uprooting) are inherently site-specific (Edmaier et al., 2011, 2015), indirectly related to flow velocity and may function via reciprocal feedbacks associated with VP-sediment dynamics (Gurnell, 2014) or interactions between VP patches (Folkard, 2005; Schnauder & Moggridge, 2009). For example, Hoyer et al. (2004)

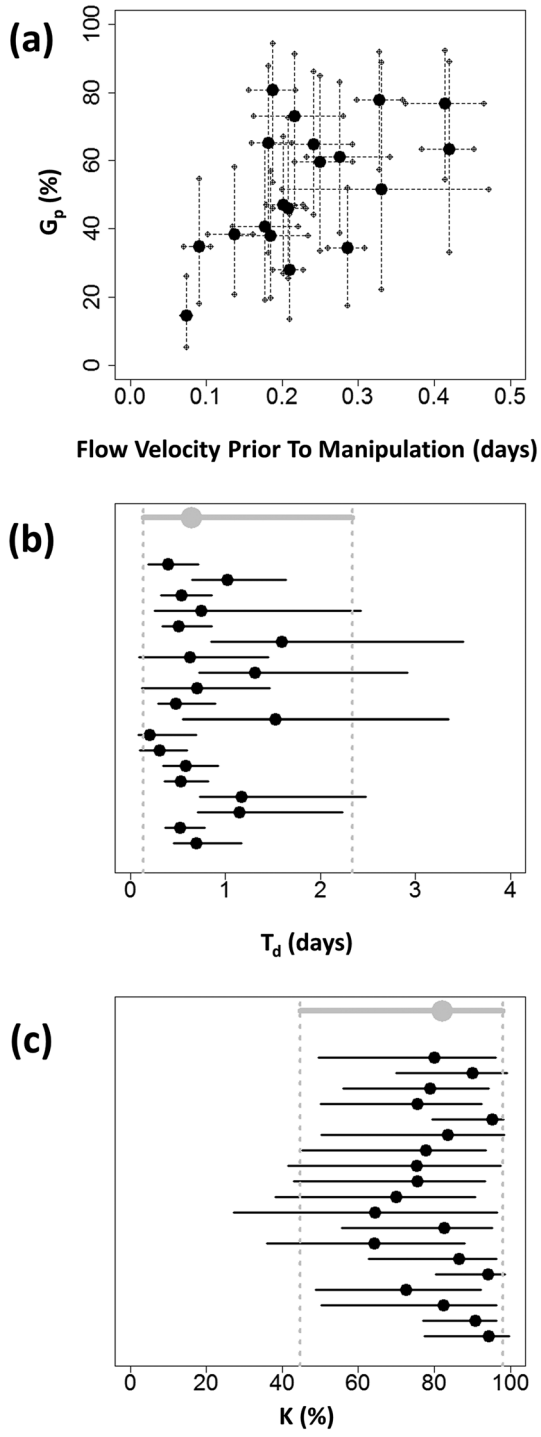

Figure 3. Results of flow manipulation experiments (n=19 deployments). In all subplots, solid circles represent median values and whiskers represent 95% credible intervals. (a) Growth potential, G_p, as a function of flow velocity. (b) Intrinsic doubling time, T_d, for each deployment (black) and the overall mixture distribution (gray). (c) The carrying capacity, K, for each deployment (black) and the overall mixture distribution (gray).

attributed the decline in VP abundance at high velocities to a lack of suitable benthic substrate for rooting, and Riis and Biggs (2003) suggested the negative relationship between velocity and VP abundance was due to uprooting or biomass loss. Both of these mechanisms are strongly dependent on near-bed hydrodynamics (e.g., shear stress), which is related to bulk flow velocity but also influenced by local morphology and vegetation conditions (Etminan et al., 2018), potentially obscuring the coherence of its effects on primary producer abundance when assessed across multiple sites (as in our study).

While the relationships between above-canopy flow velocities and near-bed hydrodynamics are modulated by vegetation and sediment properties (Marjoribanks et al., 2017), higher bulk flow velocities will usually lead to higher velocities and shear stresses near the bed. At a sufficiently large above-canopy velocities, we would thus expect near-bed hydrodynamic controls to be large enough to extirpate VP and macroalgae. The absence of such behavior in our observational data sets suggests that such extirpative velocities are rarely experienced in these spring run systems, which is consistent with their generally stable nature. Another potential reason for the discrepancies in VP and macroalgae behavior between this and other studies is variation in the quantification of abundance. This study and Riis and Biggs (2003) used percent cover, while Nilsson (1987) used species richness, and Hoyer et al. (2004) used biomass, which is not always well correlated with cover (Figures S6–S9).

The coherent hydraulic-driven control of periphyton as compared to macroalgae and VP in our study likely arises from biophysical differences in anchoring mechanisms and substrate types. The periphyton studied here typically requires VP as a substrate (Notestein et al., 2003). This places its anchoring point higher in the water column subjecting it to higher velocities and shear stresses relative to benthic macroalgae and VP under the same conditions, which anchor to the river bottom. Additionally, periphyton's VP substrate is flexible and capable of substantial motion and abrasive interactions, which can cause mechanical removal of the periphyton. Indeed, closer inspection of the King (2014) data set revealed that these observations were of macroalgae colonizing VP (and thus effectively acting as periphyton). The median macroalgae v_c estimate from this data set was 0.23 m/s and was relatively well constrained (95% CI 0.20–0.35 m/s). This velocity closely matches the values of v_c (0.22 m/s) and v_m (0.23 m/s) that we found for periphyton, which also colonizes VP; this point is discussed further below.

We augmented these observational findings using an in situ flow manipulation experiment to verify critical threshold velocity behavior for periphyton and characterize its growth dynamics when released from hydraulic-driven control. Agreement between observational and experimental findings is illustrated in Figure 3a, which shows a transition from low to high G_p at velocities above ~0.2 m/s, indicating strong growth suppression at higher velocities. This threshold-type behavior corresponds to our mean observational periphyton v_c estimate of 0.22 m/s. In combination with findings in Figures 3b and 3c, that is, rapid periphyton growth (median $T_d = 0.64$ days) and high carrying capacity (median $K = 82\%$ cover), these results indicate that without hydraulic-driven control, periphyton rapidly accumulate and reach to near-complete coverage of their host substrate. This behavior has important implications for spring ecosystems, where periphyton can directly compete with

VP for light (O'Hare, 2015; Zhang et al., 2015). Without sufficient hydraulic-driven control of periphyton, VP can be outcompeted and lost from the ecosystem (O'Hare, 2015), with broad and cascading effects across trophic levels (Choudhury et al., 2015; Duarte, 1995; UFWI, 2017). In springs exhibiting reduced flow, this process may play a major role in restructuring the PPCS. However, results from our hysteresis analysis suggest that management activities to reintroduce velocities greater than v_c in systems where periphyton has accumulated to nuisance levels can return the system to a previous state with low periphyton abundance.

Finally, we proposed the onset of continuous VP canopy motion and associated abrasive contacts within the canopy as a physical mechanism explaining critical threshold velocity behavior of algae growing on VP and estimated this velocity (v_m) from theory. It is striking how similar the theoretically derived value of v_m (0.23 m/s), is to our observationally determined periphyton v_c, experimentally determined periphyton v_c, and the v_c estimate for macroalgae growing on VP using data from King (2014; 0.22, ~0.20, and 0.23 m/s, respectively). It is likely that when macroalgae colonizes VP, it is subject to the same mechanical removal and would hence have a v_c close to that for periphyton. In short, the similarity between the suite of observational and experimental v_c estimates for algae growing on VP, and to the theoretically derived threshold for monami creation, supports the hypothesis that the initiation of continuous VP canopy motion generates the critical threshold velocity behavior in algal abundance.

Overall, this nexus of theory, observation, and experimental findings suggests that hydrodynamic controls are critical for structuring flowing-water ecosystems by shifting the competitive balance between primary producers. Explicit consideration of the interactions between primary producers and hydrodynamics, along with water quality and other anthropogenic drivers, is thus critical for developing successful ecosystem management and restoration strategies in lotic ecosystems. The multimethod approach presented here can be applied to better understand these important physical-biotic interactions in other lotic systems.

Acknowledgments
The authors declare no conflicts of interest with respect to the results of this manuscript. The data used in this manuscript are available in the SI as Data Sets S1–S3. This work was funded by the St. Johns Water Management District through the CRISPS project (contract 27789). Nathan Reaver was supported with a University of Florida Graduate Fellowship. We thank Sean King for providing data from his 2014 study, Karst Environmental Services Inc. for their role in the CRISPS SAV Groundtruthing Survey data set, Amec Foster Wheeler for their role in the Synoptic Biological Springs Study data set, two anonymous reviewers whose comments greatly improved the manuscript, and finally, Dong Joo Lee, Kevin A. Henson, Elliott E. White, Amy K. Langston, Kristen M. Reaver, Katie Glodzik, Alexa M. Mainella, Trey D. Crouch, Kimberly D. Prince, and the Watershed Ecology Laboratory for field assistance.

References

AFW (2016). Amec Foster Wheeler, Synoptic biological monitoring of springs data collection final report. St. Johns River Water Management District, St. Johns River Water Management District, Palatka, FL.

Bernhardt, E. S., Palmer, M. A., Allan, J. D., Alexander, G., Barnas, K., Brooks, S., et al. (2005). Synthesizing U.S. river restoration efforts. *Science*, *308*(5722), 636–637.

Biggs, B. J. (1996). Hydraulic habitat of plants in streams. *Regulated Rivers: Research & Management*, *12*(2-3), 131–144.

Biggs, B. J., & Stokseth, S. (1996). Hydraulic habitat suitability for periphyton in rivers. *River Research and Applications*, *12*(2-3), 251–261.

Bonn, M. A., & F. W. Bell (2003). Economic impact of selected Florida springs on surrounding local areas, Florida Department of Environmental Protection, Tallahassee, Florida, USA.

Borisova, T., A. W. Hodges, and T. J. Stevens (2014). Economic contributions and ecosystem services of springs in the lower Suwannee and Santa Fe River Basins of north-central Florida, edited, University of Florida, Food and Resource Economics Department.

Canfield Jr, D., & M. Hoyer (1988). The nutrient assimilation capacity of the Little Wekiva River, Final Report. City of Altamonte Springs, Altomonte Springs, Florida, *288*.

Casey, S. T., Cohen, M. J., Acharya, S., Kaplan, D. A., & Jawitz, J. W. (2016). Hydrologic controls on aperiodic spatial organization of the ridge–slough patterned landscape. *Hydrology and Earth System Sciences*, *20*(11), 4457–4467.

Choudhury, M. I., Yang, X., & Hansson, L. A. (2015). Stream flow velocity alters submerged macrophyte morphology and cascading interactions among associated invertebrate and periphyton assemblages. *Aquatic Botany*, *120*, 333–337.

Corenblit, D., Tabacchi, E., Steiger, J., & Gurnell, A. M. (2007). Reciprocal interactions and adjustments between fluvial landforms and vegetation dynamics in river corridors: A review of complementary approaches. *Earth-Science Reviews*, *84*(1-2), 56–86.

Doaré, O., Moulia, B., & De Langre, E. (2004). Effect of plant interaction on wind-induced crop motion. *Journal of biomechanical engineering*, *126*(2), 146–151.

Duarte, C. M. (1995). Submerged aquatic vegetation in relation to different nutrient regimes. *Ophelia*, *41*(1), 87–112.

Dunbar, J. S., Webb, S. D., & Cring, D. (1989). Culturally and naturally modified bones from a Paleoindian site in the Aucilla River, North Florida. *Bone modification*, *473-497*.

Edmaier, K., Burlando, P., & Perona, P. (2011). Mechanisms of vegetation uprooting by flow in alluvial non-cohesive sediment. *Hydrology and Earth System Sciences*, *15*(5), 1615–1627.

Edmaier, K., Crouzy, B., & Perona, P. (2015). Experimental characterization of vegetation uprooting by flow. *Journal of Geophysical Research: Biogeosciences*, *120*, 1812–1824. https://doi.org/10.1002/2014JG002898

Etminan, V., Ghisalberti, M., & Lowe, R. J. (2018). Predicting bed shear stresses in vegetated channels. *Water Resources Research*, *54*, 9187–9206. https://doi.org/10.1029/2018WR022811

Folkard, A. M. (2005). Hydrodynamics of model Posidonia oceanica patches in shallow water. *Limnology and oceanography*, *50*(5), 1592–1600.

Foss, A. J., Phlips, E. J., Yilmaz, M., & Chapman, A. (2012). Characterization of paralytic shellfish toxins from *Lyngbya wollei* dominated mats collected from two Florida springs. *Harmful Algae*, *16*, 98–107.

Franklin, P., Dunbar, M., & Whitehead, P. (2008). Flow controls on lowland river macrophytes: A review. *Sci Total Environ*, *400*(1-3), 369–378.

Frazer, T. K., Hoyer, M. V., Notestein, S. K., Hale, J. A., & Canfield, D. E. Jr (2001). Physical, chemical and vegetative characteristics of five Gulf Coast rivers, Final Report. Southwest Florida Water Management District, Brooksville, Florida, 333.
Frazer, T. K., Notestein, S. K., & Pine, W. E. Jr (2006). Changes in the physical, chemical and vegetative characteristics of the Homosassa, Chassahowitzka and Weeki Wachee Rivers, Final Report. Prepared for the Southwest Florida Water Management District. Brooksville, *FL*, 163.
FSTF, (2000). Florida's springs: Strategies for protection and restoration, Florida Department of Environmental Protection.
Ghisalberti, M., & Nepf, H. (2006). The structure of the shear layer in flows over rigid and flexible canopies. *Environmental Fluid Mechanics*, *6*(3), 277–301.
Ghisalberti, M., & Nepf, H. M. (2002). Mixing layers and coherent structures in vegetated aquatic flows. *Journal of Geophysical Research*, *107*(C2), 3011. https://doi.org/10.1029/2001JC000871
Ghosh, M., & Gaur, J. P. (1998). Current velocity and the establishment of stream algal periphyton communities. *Aquatic Botany*, *60*(1), 1–10.
Gurnell, A. (2014). Plants as river system engineers. *Earth Surface Processes and Landforms*, *39*(1), 4–25.
Hauxwell, J., Frazer, T. K., & Osenberg, C. W. (2007). An annual cycle of biomass and productivity of *Vallisneria americana* in a subtropical spring-fed estuary. *Aquatic Botany*, *87*(1), 61–68.
Heffernan, J. B. (2008). Wetlands as an alternative stable state in desert streams. *Ecology*, *89*(5), 1261–1271.
Heffernan, J. B., Cohen, M. J., Frazer, T. K., Thomas, R. G., Rayfield, T. J., Gulley, J., et al. (2010). Hydrologic and biotic influences on nitrate removal in a subtropical spring-fed river. *Limnology and Oceanography*, *55*(1), 249.
Heffernan, J. B., Liebowitz, D. M., Frazer, T. K., Evans, J. M., & Cohen, M. J. (2010). Algal blooms and the nitrogen-enrichment hypothesis in Florida springs: Evidence, alternatives, and adaptive management. *Ecological Applications*, *20*(3), 816–829.
Hensley, R. T., & Cohen, M. J. (2017). Flow reversals as a driver of ecosystem transition in Florida's springs. *Freshwater Science*, *36*(1), 14–25.
Hoyer, M., Frazer, T., & Notestein, S. (2004). Vegetative characteristics of three low-lying Florida coastal rivers in relation to flow, light, salinity and nutrients. *Hydrobiologia*, *528*(1-3), 31–43.
Huth, W. L., & Morgan, O. A. (2011). Measuring the willingness to pay for cave diving. *Marine Resource Economics*, *26*(2), 151–166.
Jowett, I. G., & Biggs, B. J. F. (2010). Flood and velocity effects on periphyton and silt accumulation in two New Zealand rivers. *New Zealand Journal of Marine and Freshwater Research*, *31*(3), 287–300.
Kail, J., Brabec, K., Poppe, M., & Januschke, K. (2015). The effect of river restoration on fish, macroinvertebrates and aquatic macrophytes: A meta-analysis. *Ecological Indicators*, *58*, 311–321.
King, S. A. (2014). Hydrodynamic control of filamentous macroalgae in a sub-tropical spring-fed river in Florida, USA. *Hydrobiologia*, *734*(1), 27–37.
Klimeš, L. (2003). Scale-dependent variation in visual estimates of grassland plant cover. *Journal of Vegetation Science*, *14*(6), 815.
Laist, D. W., & Reynolds, J. E. III (2005). Influence of power plants and other warm-water refuges on Florida manatees. *Marine Mammal Science*, *21*(4), 739–764.
Larned, S. T., Nikora, V. I., & Biggs, B. J. (2004). Mass-transfer-limited nitrogen and phosphorus uptake by stream periphyton: A conceptual model and experimental evidence. *Limnology and Oceanography*, *49*(6), 1992–2000.
Larsen, L. G., & Harvey, J. W. (2010). How vegetation and sediment transport feedbacks drive landscape change in the everglades and wetlands worldwide. *Am Nat*, *176*(3), E66–E79.
Lei, J., & Nepf, H. (2016). Impact of current speed on mass flux to a model flexible seagrass blade. *Journal of Geophysical Research: Oceans*, *121*, 4763–4776. https://doi.org/10.1002/2016JC011826
Lepš, J., & Hadincová, V. (1992). How reliable are our vegetation analyses? *Journal of Vegetation Science*, *3*(1), 119–124.
Liebowitz, D. M., Cohen, M. J., Heffernan, J. B., Korhnak, L. V., & Frazer, T. K. (2014). Environmentally-mediated consumer control of algal proliferation in Florida springs. *Freshwater Biology*, *59*(10), 2009–2023.
Malmqvist, B., & Rundle, S. (2002). Threats to the running water ecosystems of the world. *Environmental Conservation*, *29*(2), 134–153.
Marjoribanks, T. I., Hardy, R. J., Lane, S. N., & Parsons, D. R. (2017). Does the canopy mixing layer model apply to highly flexible aquatic vegetation? Insights from numerical modelling. *Environmental Fluid Mechanics*, *17*(2), 277–301.
Moss, B. (1976). The effects of fertilization and fish on community structure and biomass of aquatic macrophytes and epiphytic algal populations: An ecosystem experiment. *The Journal of Ecology*, *64*(1), 313–342. https://doi.org/10.2307/2258698
Murray, A. B., Knaapen, M. A. F., Tal, M., & Kirwan, M. L. (2008). Biomorphodynamics: Physical-biological feedbacks that shape landscapes. *Water Resources Research*, *44*, W11301. https://doi.org/10.1029/2007WR006410
Naiman, R. J., Latterell, J. J., Pettit, N. E., & Olden, J. D. (2008). Flow variability and the biophysical vitality of river systems. *Comptes Rendus Geoscience*, *340*(9-10), 629–643.
Nepf, H. M. (1999). Drag, turbulence, and diffusion in flow through emergent vegetation. *Water Resources Research*, *35*(2), 479–489. https://doi.org/10.1029/1998WR900069
Nepf, H. M. (2012a). Flow and transport in regions with aquatic vegetation. *Annual Review of Fluid Mechanics*, *44*(1), 123–142.
Nepf, H. M. (2012b). Hydrodynamics of vegetated channels. *Journal of Hydraulic Research*, *50*(3), 262–279.
Nilsson, C. (1987). Distribution of stream-edge vegetation along a gradient of current velocity. *Journal of Ecology*, *75*(2), 513–522.
Notestein, S. K., Frazer, T., Hoyer, M., & Canfield, D. (2003). Nutrient limitation of periphyton in a spring-fed, coastal stream in Florida, USA. *Journal of Aquatic Plant Management*, *41*, 57–60.
Odum, H. T. (1957). Trophic structure and productivity of Silver Springs, Florida. *Ecological monographs*, *27*(1), 55–112. https://doi.org/10.2307/1948571
O'Hare, M. T. (2015). Aquatic vegetation—Aprimer for hydrodynamic specialists. *Journal of Hydraulic Research*, *53*(6), 687–698.
Okamoto, T., Nezu, I., & Sanjou, M. (2016). Flow–vegetation interactions: Length-scale of the "monami" phenomenon. *Journal of Hydraulic Research*, *54*(3), 251–262.
Okamoto, T.-A., & Nezu, I. (2009). Turbulence structure and "monami" phenomena in flexible vegetated open-channel flows. *Journal of Hydraulic Research*, *47*(6), 798–810. https://doi.org/10.3826/jhr.2009.3536
Ortiz, X., Rival, D., & Wood, D. (2015). Forces and moments on flat plates of small aspect ratio with application to *PV* wind loads and small wind turbine blades. *Energies*, *8*(4), 2438–2453.
Patil, S., & Singh, V. (2010). Characteristics of monami wave in submerged vegetated flow. *Journal of Hydrologic Engineering*, *15*(3), 171–181.
Poff, N. L., Allan, J. D., Bain, M. B., Karr, J. R., Prestegaard, K. L., Richter, B. D., et al. (1997). The natural flow regime. *BioScience*, *47*(11), 769–784.

Poff, N. L., Richter, B. D., Arthington, A. H., Bunn, S. E., Naiman, R. J., Kendy, E., et al. (2010). The ecological limits of hydrologic alteration (ELOHA): A new framework for developing regional environmental flow standards. *Freshwater Biology*, *55*(1), 147–170. https://doi.org/10.1111/j.1365-2427.2009.02204.x

Richter, B. D., Baumgartner, J. V., Powell, J., & Braun, D. P. (1996). A method for assessing hydrologic alteration within ecosystems. *Conservation biology*, *10*(4), 1163–1174.

Riis, T., & Biggs, B. J. (2003). Hydrologic and hydraulic control of macrophyte establishment and performance in streams. *Limnology and oceanography*, *48*(4), 1488–1497.

Ryder, D. S., Watts, R. J., Nye, E., & Burns, A. (2006). Can flow velocity regulate epixylic biofilm structure in a regulated floodplain river? *Marine and Freshwater Research*, *57*(1), 29–36.

Saravia, L. A., Momo, F., & Lissin, L. D. B. (1998). Modelling periphyton dynamics in running water. *Ecological Modelling*, *114*(1), 35–47.

Schnauder, I., & Moggridge, H. L. (2009). Vegetation and hydraulic-morphological interactions at the individual plant, patch and channel scale. *Aquatic Sciences*, *71*(3), 318–330.

Scott, T. M., G. H. Means, R. P. Meegan, R. C. Means, S. Upchurch, R. Copeland, et al. (2004). Springs of Florida, edited, Florida Geological Survey, Tallahassee, FL.

Song, X., Chen, X., Stegen, J., Hammond, G., Song, H. S., Dai, H., et al. (2018). Drought conditions maximize the impact of high-frequency flow variations on thermal regimes and biogeochemical function in the hyporheic zone. *Water Resources Research*, *54*, 7361–7382. https://doi.org/10.1029/2018WR022586

Stevenson, R. J., A. Pinowska, and Y.-K. Wang (2004). Ecological condition of algae and nutrients in Florida springs, Contract Number WM, 858.

Tanino, Y., & Nepf, H. M. (2008). Laboratory investigation of mean drag in a random array of rigid, emergent cylinders. *Journal of Hydraulic Engineering*, *134*(1), 34–41.

Timpe, K., & Kaplan, D. (2017). The changing hydrology of a dammed Amazon. *Science advances*, *3*(11).

Townsend, S., Schult, J., Douglas, M., & Lautenschlager, A. (2017). Recovery of benthic primary producers from flood disturbance and its implications for an altered flow regime in a tropical savannah river (Australia). *Aquatic Botany*, *136*, 9–20.

UFWI (2017). University of Florida Water Institute Collaborative Research Initiative on Sustainability and Protection of Springs (CRISPS), St. Johns River Water Management District, Palatka, FL.

Wellnitz, T., & Rader, R. B. (2003). Mechanisms influencing community composition and succession in mountain stream periphyton: Interactions between scouring history, grazing, and irradiance. *Journal of the North American Benthological Society*, *22*(4), 528–541.

Wikum, D. A., & Shanholtzer, G. F. (1978). Application of the Braun-Blanquet cover-abundance scale for vegetation analysis in land development studies. *Environmental management*, *2*(4), 323–329.

Wohl, E., Lane, S. N., & Wilcox, A. C. (2015). The science and practice of river restoration. *Water Resources Research*, *51*, 5974–5997. https://doi.org/10.1002/2014WR016874

Zhang, C., Gao, X., Wang, L., & Chen, X. (2015). Modelling the role of epiphyton and water level for submerged macrophyte development with a modified submerged aquatic vegetation model in a shallow reservoir in China. *Ecological Engineering*, *81*, 123–132.